AN ABSTRACT OF THE THESIS OF

Alexander J. McCarthy for the degree of Master of Science in Water Resources Science and Soil Science presented on Augusts 18, 2016.

Title: The Effects of Layered Differences in Hydraulic Conductivity of Groundwater: An Estimation of Residence Time for Solute Transport.

Abstract approved:

_____

John S. Selker, Julie Pett-Ridge

In order to determine how contaminants from pharmaceutical, agriculture, and industry will move through groundwater systems, it is imperative to further our understanding of the relationship between physical, biological, and chemical properties of aquifers and transport and transformation of these products. Several studies have explored how heterogeneities in groundwater systems affect the flow and subsequent transport of solute at regional, intermediate, and local basin scales. This study expands on these studies to investigate the effects of vertically stratified differences in hydraulic conductivity on solute transport. A simple basin geometry was modeled using the finite element method. Ratios of hydraulic conductivity between the vertically stratified layers of 1, 2, 10, and 100 were simulated. In order to estimate an average residence time for the system as a whole as well as for each layer, a System Time Method was derived. This new method can be carried out a priori (relative to numerical modeling) and also allows the comparison of relative early or late time solute transport for different cases of vertically stratified hydraulic conductivity values. A method for estimating residence times in each layer also results in the ability to perform an approximation for the level of solute consumption.

The simulations of a simple basin model that were carried out in this thesis provide an initial validation of the System Time Method.

The Effects of Layered Differences in Hydraulic Conductivity of Groundwater: An Estimation of Residence Time for Solute Transport

by
Alexander J. McCarthy

A THESIS

submitted to

Oregon State University

in partial fulfillment of
the requirements for the
degree of

Master of Science

Presented August 18, 2016
Commencement June 2017

Master of Science thesis of Alexander J. McCarthy presented on August 18, 2016

APPROVED:

Co-Major Professor, representing Water Resources Science

Co-Major Professor, representing Soil Science

Director of the Water Resources Graduate Program

Head of the Department of Crop and Soil Science

Dean of the Graduate School

I understand that my thesis will become part of the permanent collection of Oregon State University libraries. My signature below authorizes release of my thesis to any reader upon request.

Alexander J. McCarthy, Author

ACKNOWLEDGEMENTS

My sincere appreciation is extended to Dr. John Selker for giving me the opportunity to learn in a challenging, supportive, and exceptionally intellectual environment. You provided me with great inspiration to always stay curious and that creativity in science knows no bounds. I would also like to thank Dr. Clément Roques, without his persistent support and guidance this project would never have succeeded. Thank you to Dr. Jack Istok for a constant willingness to work through the theory and make the process simply fun. Thank you to Dr. Julie Pett-Ridge for being a great role model as an instructor and as a scientist. I have the utmost gratitude for the group of peers that became the most indispensable friends here at Oregon State University as well as into the rest of life. Your encouragement allowed me to reach this potential. Most importantly, I have to thank my mother. Through times of hardship and uncertainty you have always shown me love and support.

In memory of my late father.

TABLE OF CONTENTS

LIST OF FIGURES

LIST OF TABLES

Chapter 1. Introduction and Context

Groundwater accounts for approximately 30% of all freshwater on Earth (USGS, 2016). While the majority of freshwater is inaccessible in glaciers and ice caps, the volume of water stored in the subsurface is about 100 times greater than that of fresh water stored in lakes and rivers. Groundwater provides drinking water for 1.5 billion people worldwide and more than half the population of the United States (Alley et al., 2002; Nolan, 2000). Even though the distribution of industry and agriculture depend largely on the availability and access to clean freshwater, an abundance of instances of groundwater contamination have occurred in the United States and around the world (Pye and Jocelyn, 1984). Since the establishment of the Comprehensive Environmental Response, Compensation, and Liability act of 1980 (CERCLA, 1986), considerable effort has been put forth to study, prevent, and remediate contaminated groundwater sites. However, the continued growth in the industrial and agricultural sectors of the United States has led to researchers documenting an increase in the frequency of chemical and microbial constituents that adversely alter the quality of fresh groundwater (USGS, 2016). This new wave of contamination is due to chemical and biological species that have not historically been considered contaminants. Constituents that are now being classified as emerging contaminants, range from pharmaceuticals to personal care products to agricultural products (Raghav et al., 2013). As the number of contaminants that enter our freshwater stores continues to rise, it is becoming increasingly important to understand the interaction between physical, biological, and chemical processes occurring in groundwater systems.

Research in the interdisciplinary field of subsurface contaminant fate and transport is extremely challenging due to difficulties in obtaining high resolution data as a result of the large degree of heterogeneity in physical, biological, and chemical properties of groundwater systems.

Chapter 1. Introduction and Context

Studies of contaminants or other foreign substances that alter the composition of groundwater systems can be conducted through field experiments, batch/column experiments carried out in the laboratory, and numerical modeling simulations. Of these methods, numerical modeling is often used as it provides immediate visualization of both spatial and temporal scales and can provide guidance in field data collection (MacQuarrie and Mayer, 2005). With the use of automatic calibration schemes, uncertainty analysis, and computer visualization tools, it has become more accessible to study and understand the effects of variable aquifer properties on groundwater flow patterns (Alley, 2002). Recent studies that have implemented numerical modeling techniques to simulate reactive transport have been aimed at determining how the residence time of groundwater systems is related to solute transport (Cardenas and Jiang, 2010; Cardenas, 2007, 2008; Haggerty et al., 2000; Haggerty et al., 2004; Jiang et al., 2010; Jiang et al., 2009).

The time it takes a parcel of water to travel through a subsurface system is especially important in determining the movement of contaminants through groundwater. Hydraulic conductivity is a frequently measured parameter in subsurface systems and can be used to differentiate soil or geological units. Due to the variability in regional geomorphological processes, groundwater basins contain units that are heterogeneous in hydraulic conductivity. Often times aquifers are made up of horizontally oriented layers with contrasting hydraulic conductivity. The velocity of water in groundwater systems, and subsequently the residence time of that water, is highly influenced by the hydraulic conductivity (Haggerty et al., 2004).

Chapter 1. Introduction and Context

How do vertically stratified differences in hydraulic conductivity affect the residence time of solute being transported through a groundwater basin? This thesis will answer this question by conducting numerical simulations consisting of steady-state and time dependent aspects. In doing so, this study will conduct an initial validation for a novel analytical method to estimate average residence times globally and within each vertically stratified layer which employs readily available data based on simple geometric features of the system.

Chapter 2. Literature Review

Due to the complexities involved with implementing numerical models to simulate processes occurring in natural systems, we must first consider the current state of the art. Doing so will allows us to incorporate the assumptions necessary to make analysis and interpretation feasible when conducting simulations that couple physical and reactive processes. This chapter will focus on summarizing the theory behind reactive transport while also providing examples of studies where this theory has been applied with the addition of certain complexities that provide a more realistic representation of natural sub-surface systems.

A common and feasible method for investigating sub-surface solute transport is the control volume approach to derivation of the advection-dispersion equation. A simple representation of the control volume method is shown in figure 2.1. This approach allows the representation of geometry, hydraulic conductivity, and flow velocity/volumetric discharge in the form of a governing differential equation. The equation contains a parameter referred to as the dispersivity to represent the processes contributing to smearing of the contamination during transport. It is possible to determine the effective macro-scale longitudinal dispersivity of the system by introducing a single pulse of conservative tracer and recording the evolution of concentration with time at the outlet. Since such experiments would be inordinately expensive and time consuming to conduct in the field, laboratory-based column experiments are typically employed in the estimation of parameter values found in the advection-dispersion equation. Beyond cost and time, this is also due to the fact that the column material can be prepared to be homogeneous where properties of the material and transport/transformation of target compounds can be directly measured (Huang et al., 1994). When numerical modeling is implemented, approximate solutions to the advection dispersion equation may be obtained through a variety of

numerical methods, including explicit finite element schemes (USGS, 2016). The chemical interaction of target compounds is subsequently calculated from the transport portion and is the sum of all the equilibrium and non-equilibrium reaction rates. In other words, with each time step, first advective transport is calculated, then all equilibrium and kinetically controlled reactions are resolved (USGS, 2016).

The constant volume approach and column experiments have been used in several studies as an attempt to simplify geologic heterogeneities. This approach can be used to study systems that are heterogenous in 1,2, and 3 dimensions as illustrated in work by Illangeskare et al. in 1995. However, flow through subsurface systems does not occur in a perfectly rectangular geometry.

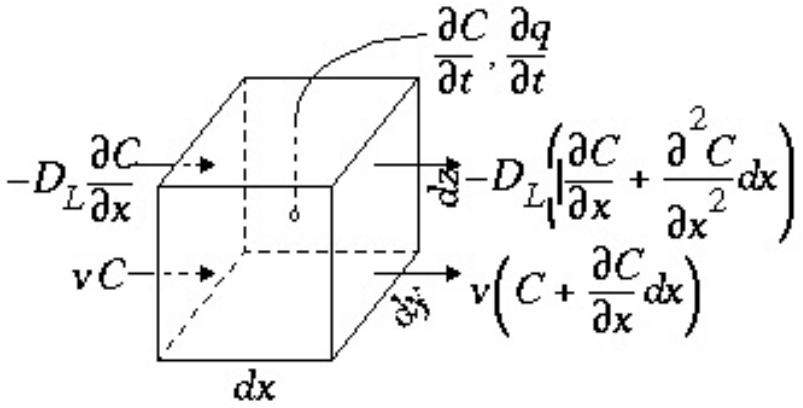

Figure 2.1 Illustration of the control volume approach, here with the x-axis aligned with the direction of flow, that is often employed to derive the advection-dispersion equation based on conservation of mass and Fick's law (note: degradation is not included in this representation so as to retain simplicity of the figure, but is typically accounted for as well).

An initial complexity to consider when studying sub-surface systems is a more realistic change in the surface topography and the subsequent change in the topography of the groundwater table. The addition of this complexity allows analysis of sub-surface systems on a range of temporal

scales. The addition of variations in water table topography even in simple groundwater systems give rise to an extreme distribution of transport velocities. Recent studies have given significant attention to subsurface flow at regional, intermediate, and local scales by applying a non-linear change in topography to represent flow in a groundwater basin (Cardenas and Jiang, 2010; Jiang et al., 2010; Toth, 1963). In 1963, Toth developed a geometry that would allow for the interpretation of groundwater flow at multiple spatial and temporal scales. Toth considered the location and extent of recharge and discharge areas, the direction and velocity of flow at any give point in the region, and the depths of penetration of the flow systems to be the three most important features to understand the movement of groundwater (Toth, 1963). He went on to discuss the development of an idealized regional basins as well as the theoretical method to work from large basins to small basins. Toth defined a small basin as:

> An area bounded by topographic highs, its lowest part being occupied by an impounded body of surface water or by the outlet of a relatively low order stream and having similar physiographic properties over the whole of it's surface.

This description of a local basin is important as it details how to define the boundaries of flow in a regional basin. One of the assumptions that has carried over into studies conducted with the Toth basin model as a foundation is that "the water table is generally similar in form to the land surface." These boundary conditions allowed Toth to compare the flow of large basins where negligible local relief results in a general slope across the regional basin against the flow of a topography that has a well defined relief at the local scale resulting in topographic lows and highs along the regional basin. Toth found that a well-defined relief results in local flow systems originating compared to a regional flow system that develops when the slope in topography is linear. Toth concluded that at the boundary between two local basin portions of a regional basin,

the flow is subvertical in either the downward or upward direction and is related to recharge and discharge areas respectively.

Cardenas (2007) sought to build on Toth's concept of how surface and groundwater are interconnected at the regional scale by employing this framework to make predictions of stream chemistry. Cardenas states that the power-law residence time distributions (PLRTDs) had normally been attributed to heterogeneity in groundwater, but that these PLRTDs can result from regional topographies where subsurface properties are homogeneous. Cardenas' study investigated the fractal behavior of solute transport in groundwater and how that affects stream chemistry. This behavior results in contaminant loads being initially flushed out but leaving behind a persistent low-level tail in contamination. In terms of the Toth basin, this is due to an upper zone of active flow, an intermediate zone of delayed flow, and a lower zone of relatively stagnant water. The concentration that is discharged into the stream scales with these zones of flow. Cardenas further summarizes the distribution of flow path length throughout the Toth basin geometry. He states that flow path lengths range from infinitesimal at the hinge lines (an imaginary longitudinal line that separates the recharge area from the discharge area) to long flow paths that go towards stagnation zone. Even when considering a homogeneous aquifer, longer flow paths in classical Toth basin geometries result in late-arrival times of solute and give the residence time distributions a multi-modal shape. The late-arrival times in Cardenas' work were five orders of magnitude larger than the early-arrival times along short flow paths. In this work, Cardenas considers differences in dispersivity in order to analyze the Toth-style flow field, but does not take into account heterogeneities in hydraulic conductivity.

Chapter 2. Literature Review

Structured heterogeneity has been explored in many sub-surface flow studies, typically taking hydraulic conductivity to decrease with depth below the surface (e.g., Selker et al., 1999; Rupp and Selker, 2005). Similarly, Jiang et al. (2010) and Jiang et al. (2009) revisited the same Toth basin geometry considering the effects of decaying hydraulic conductivity with depth on regional groundwater flow. To investigate this relationship, the authors compared the development of flow systems with different decay exponents for hydraulic conductivity. Jiang and Cardenas (Cardenas and Jiang, 2010) found that local flow systems actually penetrate deeper with greater decay in hydraulic conductivity resulting in regional flow systems becoming diminished. They also found that the rate of total recharge into the system, decreases with increasing hydraulic conductivity decay and is subsequently controlled more by the local relief of the water table and topography (Jiang et al., 2009). A similar study by Jiang in 2010 found that "depth-decaying K mostly leads to aging everywhere in the basin with the aging systematically increasing with depth, which reflects the increased residence time due to pronounced deceleration with depth" (Jiang et al., 2010). Aging is defined as an increase in the amount of time taken for a solute, and inherently the parcel of water carrying the solute, to reach the discharge area along a particular flow path relative to a homogeneous case. Therefore, when the rate of decay in hydraulic conductivity with depth is increased, the residence time along any flow path through a groundwater system increases.

The most recent study by Cardenas and Jiang (2010) regarding regional basin groundwater flow aimed at combining the past three studies with depth decaying permeability and porosity in both a simple basin geometry and the Toth regional basin geometry. Cardenas and Jiang (2010) found similar results to the previous studies stating "additional and combined

effects of heterogeneity and basin geometry on the generation of power law RTDs." The authors go on to discuss the resultant effect of large-scale heterogeneities where slow flowing zones at depth are enlarged and flows near the land surface are accelerated.

Throughout their studies Cardenas and Jiang used a specific method to nondimensionalize time in order to interpret the transport outcomes of these problems across multiple temporal and spatial scales. The method used by the two authors is explicitly discussed in Cardenas' study from 2007 where he analyzed residence time distributions of "Toth flow". Using an average Darcy velocity magnitude (in meters per second) and the horizontal length of the system in question (in meters), Cardenas was able to nondimensionalize time by calculating the product of each specific time step of the simulation with the Darcy velocity magnitude as a proportion of the length of the domain (Cardenas, 2007). Cardenas and Jiang denote this nondimensionalized residence time value as τ. When τ =1, the corresponding time step reflects the mean time needed for solute to be transported through the entire system and can be considered the residence time of that system. This method for nondimensionalization allowed the studies of Cardenas and Jiang to compare relative times for systems where parameters controlling flow were altered. A significant shortcoming of the method proposed is that the τ values can only be determined through numerical simulations where an average Darcy velocity magnitude is generated. In other words, this method does not allow for the determination of the residence time of a groundwater basin without the implementation of a numerical model. This method provided a large impetus for this study as we considered it valuable to be able to determine residence time without the use of simulations and based on intrinsic characteristics of the basin (Cardenas and Jiang, 2010; Steefel et al., 2005). As a result of our consideration of the

current state of the art, our objectives are to (1) develop a method to calculate an estimate of residence times in each layer *a priori*, (2) develop a numerical model to investigate the effects of vertically stratified differences in hydraulic conductivity in groundwater on residence time, and (3) to investigate the effects of the relationship between chemical reactions of solute and physical heterogeneities on solute transport times.

Chapter 3. Methodology

3.1 Introduction

In order to test our ideas about developing an analytical estimate of residence and transport times, it is necessary to have a numerical solution to which we can compare our predictions. Therefore, to investigate how vertically stratified differences in hydraulic conductivity affect the residence time of solute being transported through a groundwater basin, numerical flow and transport simulations were conducted using the finite element model COMSOL Multiphysics (Version 5.2, COMSOL, Inc., Burlington, Ma.). In COMSOL, the workflow involves specifying a geometry, defining all of the necessary materials, and physics, meshing and solving the model, and visualizing and post-processing the results. The specific steps used to develop the mathematical model used in this research will be discussed here.

3.2 System Geometry:

The geometry of the modeled basin we employed is similar to that used by Jiang et al. (2010) and Cardenas (2007, 2008). The basin is a 2-dimensional domain with rectangular lower boundaries and bounded at the top with half-cycle sinusoidal shaped top boundary that represents both the ground surface and the water table (i.e., maintaining a constant zero-pressure boundary condition at the soil surface, which can support either in or out-flow). Our initial assumption is consistent with Jiang et al. (2010) where the average level of the water table is considered constant for a two dimensional cross-section of a basin and is parallel to the change in topography under natural equilibrium conditions. All other boundaries are considered no-flow boundaries. This simple basin model results in the higher half of the top boundary acting as a recharge area and the lower half as a discharge area. Both the recharge and discharge areas are

considered to be at steady-state. We consider a single unit basin geometry with upper boundary defined by:

$$z_s(x) = z_0 + a\cos(\frac{2\pi x}{\lambda}) \quad (1)$$

Where:

z_0 =height of mid-point(m)

a =amplitude of variations (m)

$\boldsymbol{\lambda}$ =wavelength of periodic topographic variation

x =horizontal distance from the origin

This equation indicates that the water table has an elevation of $z_s(x)$ and is equivalent to the specific head boundary condition $h(x, z_s)$. z_0 is representative of the height at the mid-point of the site. a is the amplitude of variations and is the value that dictates the amplitude of the sinusoidal curve. $\boldsymbol{\lambda}$ is the wavelength of periodic topographic variation and controls the minimum and maximum height of the domain. x is the horizontal distance from the origin and has a maximum value equal to half of $\boldsymbol{\lambda}$.

Equation 1 is used to define the change in topography of the top boundary as well as a constant head boundary.

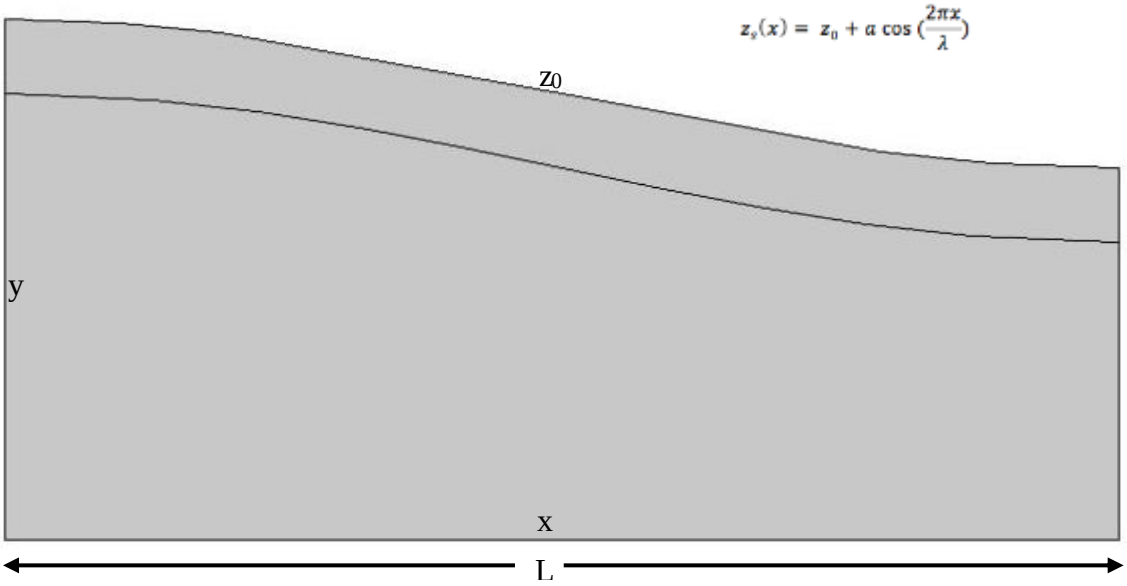

Figure 3.1: Simulated Basin Domain Geometry.Equation 1 also serves a third purpose; it is taken as the shape of the boundary between the top and bottom layers of the domain. For this boundary, all parameters in equation 1 are held constant except for the height at the origin (z_0). z_0 can be offset by a constant depth along the entire horizontal distance of the domain. The thickness of the top layer (T_1) is therefore dependent on how much z_0 is offset. For the purpose of this study, the desired thickness of the top layer is set so that:

$$T_1 = 0.2 \cdot z_0 \tag{2}$$

This results in a boundary between the top and bottom layer that parallels the constant head boundary ~20% below the constant head boundary. As a result, these layers are vertically stratified throughout the length of the domain. The use of equation 1 to establish the domain geometry and boundary between layers is illustrated in figure 3.1. A table listing all parameter values to establish the geometry of the domain can be found in Appendix A.

3.3 Material

To conduct a numerical simulation, the properties of the aquifer materials must be specified. Water is taken to fill all pore space (i.e., there is no gas or unsaturated media in this domain). The porosity of the system was taken to be a constant of 0.2. Due to the constant zero pressure head boundary condition, the system automatically remained saturated in our simulations.

3.4 Governing Equations and Model Simulations

In order to perform simulations using COMSOL Multiphysics, the user is prompted to *'add physics.'* The user assigns a specific set of equations that control the simulation either at steady-state or on a time dependent basis. The equations used for the steady-state flow portion and the time dependent transport of a diluted species through porous medium are discussed below.

3.4.1 Steady-State Simulations (Darcy's Law):

The hydraulic head boundary condition ($H(x, z_s)$), no flow boundary condition, hydraulic conductivity values, and subsequent pressure field generated from the geometry control the flow direction through the domain. The governing equation for the steady-state flow through the domain is Darcy's Law.

Darcy's Law:

$$q = -K \cdot \nabla H \tag{3}$$

$$v = \frac{q}{n} \tag{4}$$

Where:

K =hydraulic conductivity(Lt^{-1})

H =hydraulic head(L)

q =Darcy velocity (Lt^{-1})

v =seepage velocity(Lt^{-1})

n =porosity

However, the domain is represented in a 2-Dimensional space. Therefore, we only need to consider the specific discharge in the x and y directions:

$$q_x = -K_x \frac{\partial h}{\partial x} \tag{5}$$

$$q_y = -K_y \frac{\partial h}{\partial y} \tag{6}$$

Other than the sinusoidally-varying head upper boundary, all other boundaries were taken to be no-flow boundaries. No-flow boundaries can be represented by the following equations:

$$-n \cdot \rho q = 0 \tag{7}$$

Where:

n =the vector normal to the boundary

ρ =the density of the fluid (Kg/m^3)

Equation 1 was used to divide the domain into two vertically stratified layers. The governing equations require the selection of a hydraulic conductivity value (K in m/d). COMSOL allows each layer to receive a specific value for K. From this point forward the

hydraulic conductivity in the top and bottom layers is denoted by K_1 and K_2 respectively. An initial value of K was selected and applied to the whole domain. Subsequent simulations were run for four cases where the ratio of K_1:K_2 is increased. The following ratios of K_1:K_2 represent each of the four cases: 1:1, 2:1, 10:1, and 100:1. The table of the specific values used can be found in Appendix A. The hydraulic conductivity in each layer is isotropic in the x and y directions. The steady-state flow simulations result in one constant hydraulic head distribution but four different velocity distributions.

3.4.2. Time-Dependent Simulations (Transport of Diluted Species in Porous Media): The equations in the Transport of Diluted Species in Porous Media use the Darcy Velocity outputs from the steady-state simulations to drive the transport in time. The governing equation used to simulate transport is a simple (no degradation or sorption) form of the advection dispersion equation:

$$\frac{\partial c_i}{\partial t} = \nabla \cdot (D_i c_i) - q \cdot \nabla c_i \qquad (8)$$

Where:

c_i =concentration of species i (mols)

t =time

D_i =dispersion coefficient (L^2t^{-1})

q =local velocity (Lt^{-1})

The advection-dispersion equation allows for the determination of the change in concentration with the change in time and space. The model output data records concentration with time at each node of the finite element mesh. In order to determine the diffusion coefficient (which has a single value throughout the domain), COMSOL uses the Millington and Quirk model. This model takes into account the porosity as well as the degree of saturation of the system in order to determine the tortuosity and cross-sectional area available for the movement of solute (Saripalli et al., 2002). We must define solute boundary conditions for the advection-dispersion equation. As mentioned in chapter 3.2, the constant head boundary controls the flow and results in the top half of this boundary representing a recharge zone and the bottom half representing a discharge area. As a result, this boundary is partitioned so that the recharge area reflects the source of solute (i.e. source of contamination) and the discharge area represents the destination of the solute (i.e. here taken to discharge into an imagined river). In order to normalize the concentration of solute when analyzing data, the recharge area was given a constant concentration of 1 mol/m^3; this is considered a Dirichlet boundary condition. The discharge area occurs at the lower half of the constant head boundary and acts as an area of outflow where solute is transported out of the model domain as function of fluid motion. All other boundaries (sides and bottom) are set to be no flux boundaries where no mass flows in our out. The initial concentration within the domain was set to be 0 mol/m^3.

Averaging was applied to the discharge to present the flow-weighted average concentration (mol/m^3) of the solute at each time step at the outflow boundary. This

represented the instantaneous translation of any fluid leaving the sub-surface to the imagined riverine receiving body, supposing that movement upon emergence to the surface is essentially instantaneous in comparison to subsurface flow. This allows for dimensionless comparison between the flux of solute leaving the system to the flux of solute that entered the system (e.g., mass in versus mass out, or concentration in versus concentration out).

Initial transport simulations were conducted for a conservative tracer (i.e., no degradation and no sorption). Simulations to evaluate the evolution of concentration of solute with time were conducted for the same four cases of ratios of hydraulic conductivity between the top and bottom layers as discussed in section 3.4.1 of this text.

In order to investigate the relationship between vertically stratified differences in hydraulic conductivity and solute transport, reaction rates were subsequently taken into account. For this study, only first order rate constants were considered. First order rate constants follow the general formula of:

$$\frac{-dc_i}{dt} \equiv r = kc_i \tag{9}$$

Where:

c_i =concentration of species i (mols)

t =time

r =reaction rate (mols t^{-1})

k =first order rate constant (t^{-1})

The addition of a reaction rate to the solute transport physics in COMSOL results in the advection dispersion equation gaining a term:

$$\frac{\partial c_i}{\partial t} = \nabla \cdot (D_i c_i) - q \cdot \nabla c_i - k \cdot c_i \quad (10)$$

Rate constants were calculated through use of the Damköhler number (Da). The Damköhler number relates the reaction timescale to the advection timescale and can be used to determine if reaction rates or advection rates dominate in a system. A general rule of thumb is that for Da <<1, advection occurs much faster than the reaction and for Da>>1, the reaction rate is greater than the advection rate; and most of the solute is consumed (Fitzgerald, 2001). The Damköhler number is calculated as follows:

$$Da = k \cdot c_0^{n-1} \cdot \tau \quad (11)$$

Where:

k =reaction rate constant (t^{-1})

c_0 =initial concentration (mols)

n =reaction order

τ =mean residence time (t)

This equation is considered to be dimensionless because it can be simplified to:

$$Da = \frac{reactive\ rate}{convective\ mass\ transport\ rate} \quad (12)$$

By setting the Damköhler number to a certain value with an initial concentration of zero, it is possible to rearrange equation 11 to solve for a specific first order rate constant. The Damköhler number for the bottom layer was held constant at 0.1. Reaction rates for the top layer were calculated for all four cases of K_1:K_2 and for Damköhler numbers of 0.1 and 10. In other words, each case of K_1:K_2 was simulated for two scenarios of Da_1:Da_2

(where Da_1 and Da_2 is the Damköhler number in the top and bottom layers respectively): 1:1 and 1:100.

3.5 Discretization

The finite element analysis method requires a user defined discretization in order to solve for the partial differential equations used in groundwater modelling. COMSOL creates a mesh for discretization once the geometry and physics have been established. The size of the individual mesh units is calibrated for fluid dynamics and is based on the Péclet number. The Péclet number is dimensionless ratio of contributions to mass transport by convection to those by diffusion over a certain characteristic length scale. When the characteristic length scale is very large, the Péclet number is much greater than one and convective processes dominate while diffusive contribution is considered negligible. When using the finite element method, the size of the mesh is representative of the characteristic length scale. Therefore, in order to minimize error and ensure that diffusive processes are taken into account, the mesh is refined throughout the domain. This results in a mesh that is sufficiently fine to provide an accurate stable solution.

Chapter 4. Results and Discussion

4.1 Introduction

This chapter analyzes and discusses the results derived from each steady-state simulation as well as the subsequent time-dependent simulations of solute transport. It is necessary to initially determine if each simulation is producing the expected flow field based on the parameters that control flow. Using the steady-state simulations we then derive a novel method for estimating the average residence time of the system and the average residence time for each layer a priori. The solute transport models without degradation or sorption (i.e., a conservative tracer) are then used as an initial validation for our developed method. This method for estimating average residence times is then applied to the analysis of simulations where solute is transformed through reactive processes.

4.2 Steady-State Analysis

The initial output of the simulations is a hydraulic head distribution of the domain (figure 4.1). As mentioned in chapter 3.2, the top boundary is a constant head boundary and therefore controls flow throughout the system. The hydraulic head gradient is distributed along the top boundary with the maximum hydraulic head value located at the topographical high and the minimum hydraulic head value located at the topographic low. The parameters that govern the constant head boundary remain constant throughout each simulation of K_1:K_2. Figure 4.1 illustrates the hydraulic head distribution for each simulation and serves as a verification that the steady-state flow simulations are what would be expected

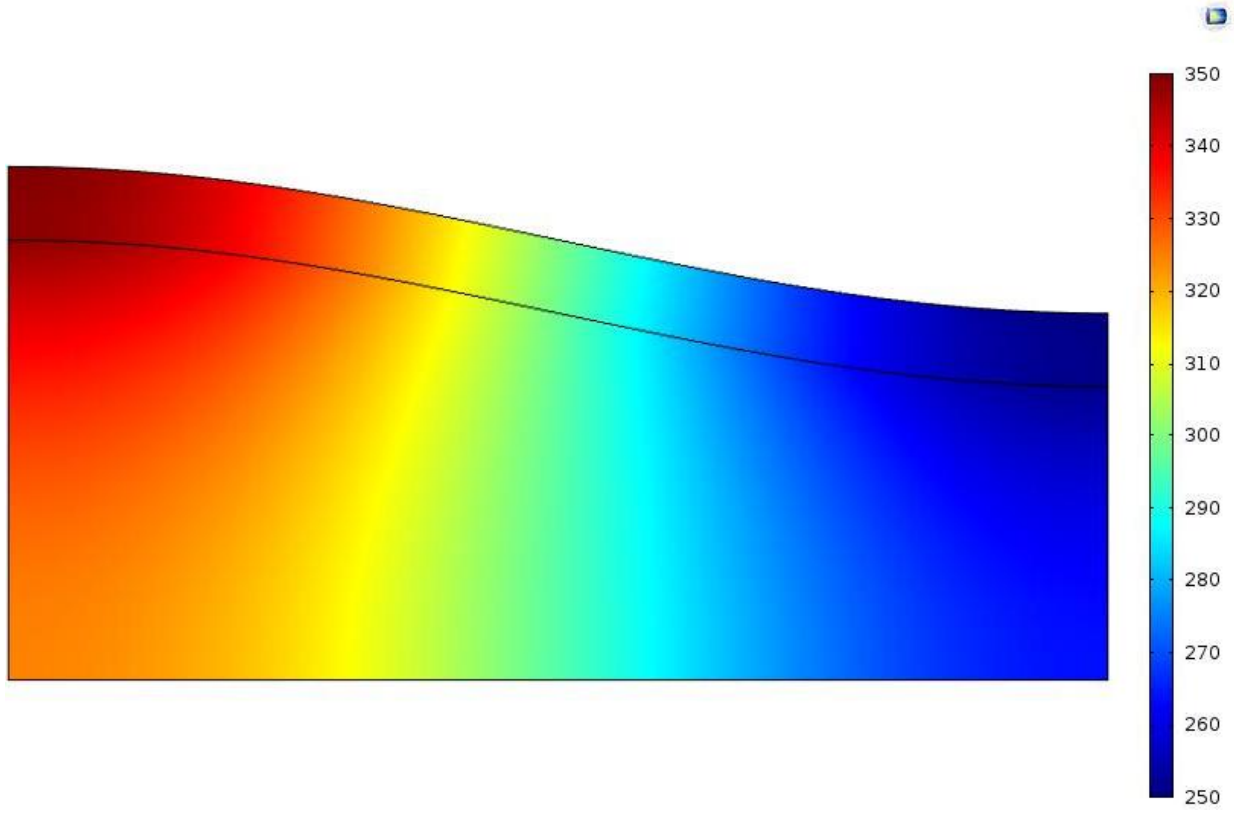

Figure 4.1: Hydraulic Head Distribution in m for the modeled domain.

The Darcy velocity (q) depends on hydraulic conductivity and the gradient of hydraulic head (which at the upper boundary is identical in all of the simulations of this thesis) (eq 3; figure 4.2). The maximum rate of change in groundwater velocities are concentrated at the divide between the recharge and discharge areas, and at the interface between the two aquifer materials (figure 4.1). This area is where the hydraulic head gradient is largest. In the homogeneous case, where K_1:K_2 is 1:1, the frequency distribution of velocities follows a smooth distribution as seen in figure 4.2. As K_1 increases, the distribution of velocities in the bottom layer stay the same, but there is an increase in the frequency of velocities in the top layer

that are much greater than those in the bottom layer. Figure 4.2 plots the frequency distribution of average Darcy velocity for each case. All four cases exhibit a normal frequency distribution around the intermediate Darcy velocities that are concentrated in what can be considered the middle of the domain. As K_1 increases there is an increase in velocity in the top layer resulting in a second distribution of velocities that is much greater than those in the bottom layer. This is especially evident in Figure 4.2 for K_1:K_2 of 100:1 where the frequency of the intermediate velocities have decreased relative to the 1:1 case but there is the presence of a second distribution of velocities that are much greater. Figure 4.3 shows the linear correlation between the average Darcy Velocity in the domain and the hydraulic conductivity in the bottom layer.

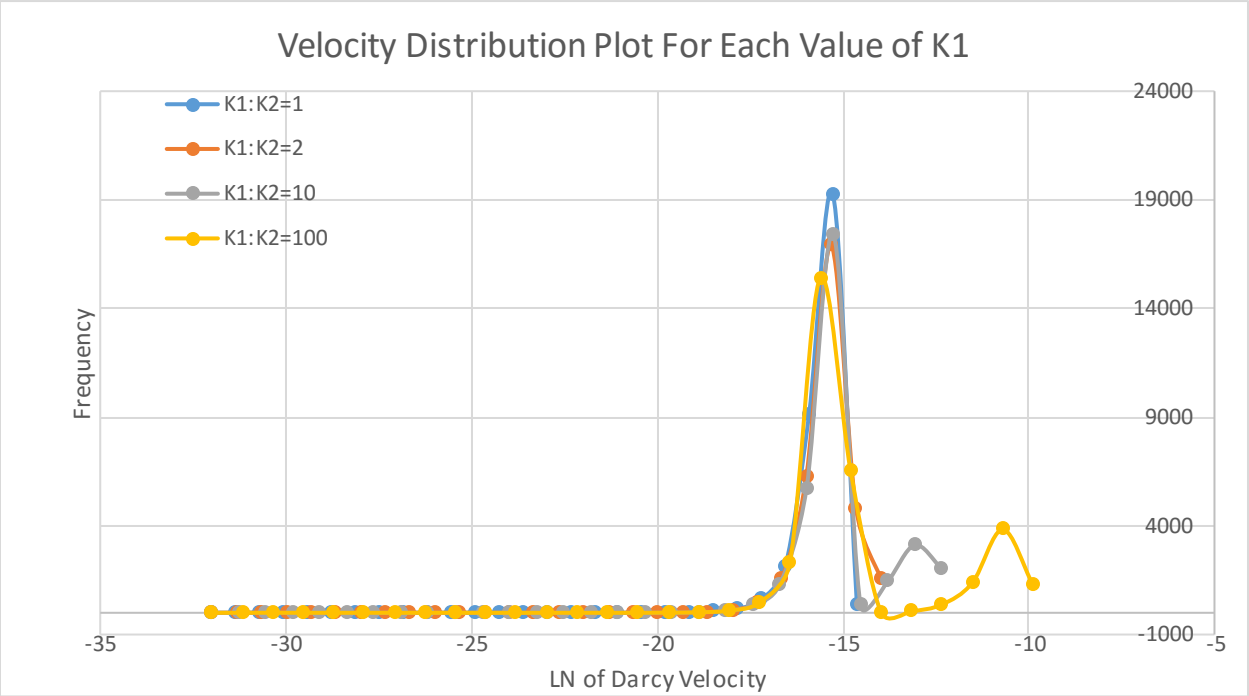

Figure 4.2: Frequency Distribution of the Natural Log of Darcy Velocity (m/s) for each case.

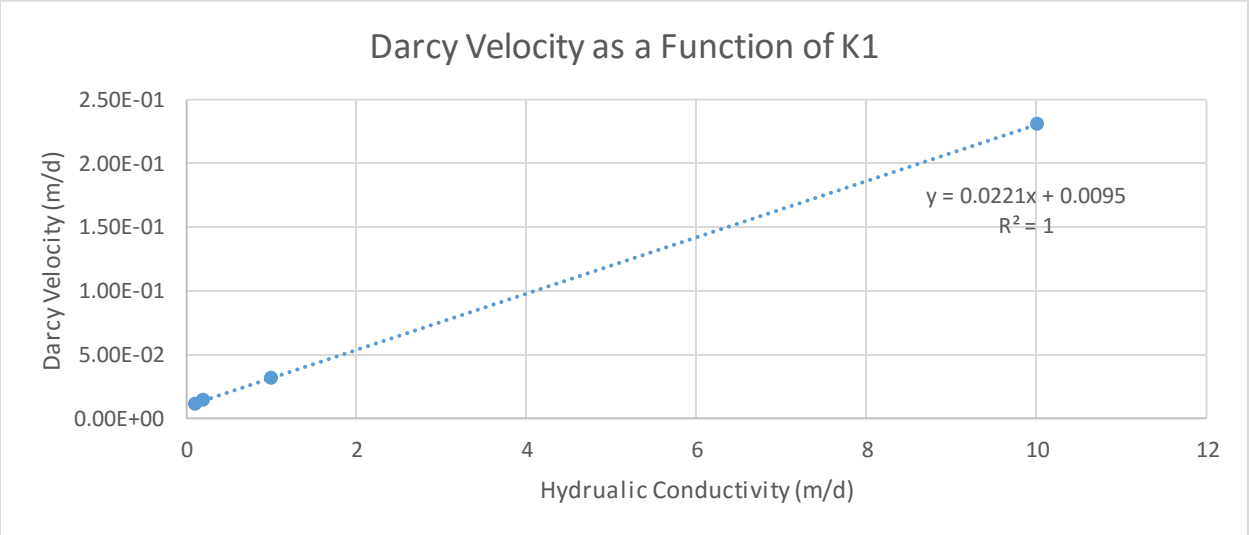

Figure 4.3: Darcy Velocity as a Function of K1.

Each velocity distribution in figure 4.4 has 25 stream lines where each stream tube is representative of 4% of the total volumetric discharge. Figure 4.4a represents the homogenous case for hydraulic conductivity and as a result, the streamlines are equally distributed throughout the domain. As K_1 increases, more and more of the streamlines become distributed in the the top layer. In fact, almost all of the stream tubes in the K_1:K_2 case of 100:1 travel through the top layer resulting in >90% of the volumetric flow being contributed from this layer. The increase in velocities in the top layer results in a much greater proportion of the volumetric discharge flowing through the top layer. Cardenas (2007) notes similar phenomenon when modeling the Toth Basin where "the flow path lengths vary from an infinitesimal length along the hingelines to flow paths that go towards stagnation zones." Cardenas goes on to state that "shorter path lengths also have higher Darcy velocity while the longer flow paths go through areas with much smaller Darcy velocity" (Cardenas, 2007). Therefore, increasing the difference in hydraulic conductivity between the top and bottom layer in a simple basin model results in the deeper circulation becoming relatively weakened while the shallow circulation becomes enhanced (Cardenas, 2010). This in turn will affect the mean residence time of the top layer as a greater amount of water is flowing through that area of the domain at a much faster rate.

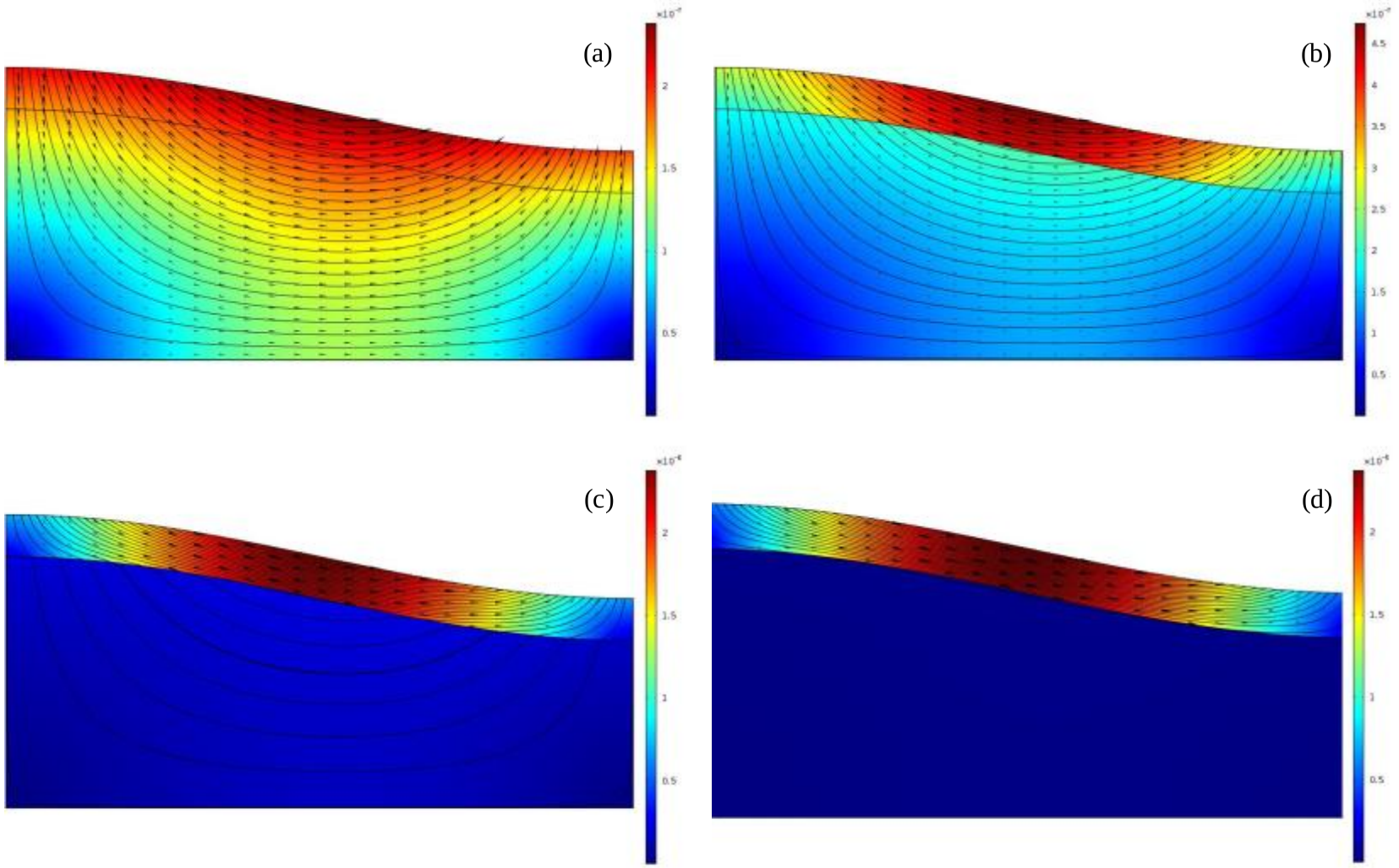

Figure 4.4: Darcy Velocity Distributions in m/s for each scenario. (a) K_1:K_2=1 (b) K_1:K_2=2 (c) K_1:K_2=10 (d) K_1:K_2=100

4.3 Derivation of the System Time Method

The Cardenas method (Cardenas 2007; Cardenas and Jiang, 2010), as discussed in Chapter 2, nondimensionalized time by using the average Darcy velocity magnitude and the horizontal length of the domain. This nondimensionalization is calculated through:

$$\tau = \frac{t \cdot q}{L} \tag{13}$$

Where:

τ =the characteristic flushing time (t)

t =time (t)

q =average Darcy velocity magnitude ($L\ t^{-1}$)

L =length of the domain (L)

When τ is equal to one, the equivalent time is representative of the characteristic flushing time or the amount of time required for one pore volume of water to move through the system. τ is also a function of the average Darcy velocity of the whole system as well as the length of the system or domain. However, this expression for residence time does not take into account the differences in Darcy velocity distributions as a result of hydraulic conductivity heterogeneities. Furthermore, Cardenas uses the average Darcy velocity for a homogenous case that is retrieved post-simulation using COMSOL Multiphysics. It is for this reason that we propose a simple method to estimate a mean residence time as well as layer specific residence times that can be carried out a priori.

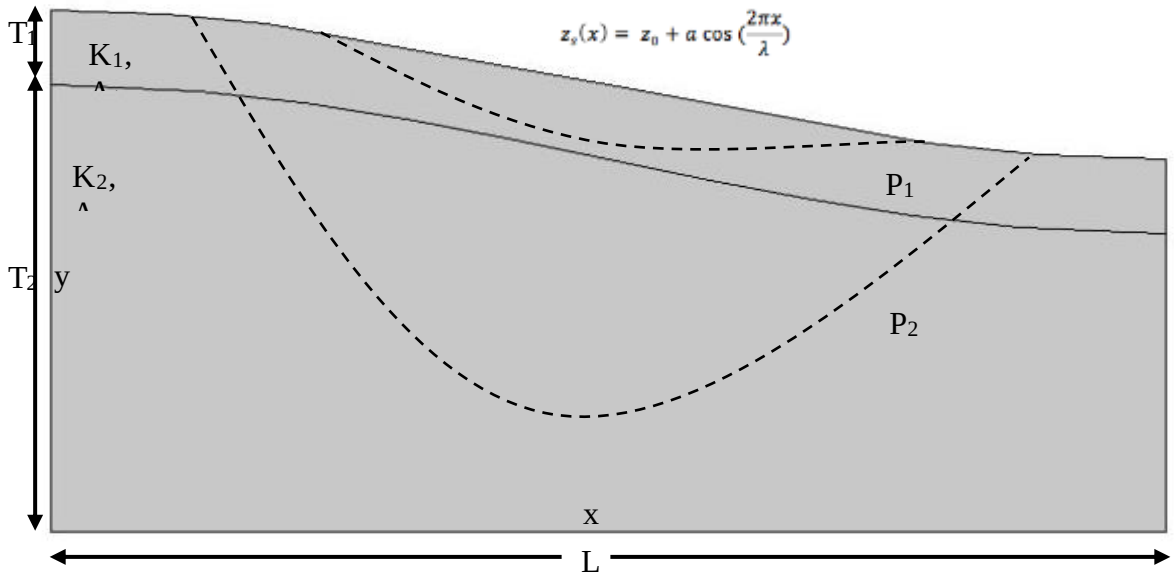

Figure 4.5: Idealized groundwater basin with system properties.

Figure 4.5 illustrates the idealized groundwater basin used throughout our simulations as well as the geometry that will be used to develop the residence time estimates. The parameters that are identified within this geometry are denoted as system properties and are considered intrinsic to the system. These parameters are defined as follows:

T_1 =thickness of the top layer

T_2 =thickness of the bottom layer

L =length of the domain

A_1 =area of the top layer

A_2 =area of the bottom layer

P_1 =average length of the flow-path through the top layer

P_2 =average length of the flow-path through the bottom layer

Chapter 4. Results and Discussion

Although the values used for the subsequent simulations were selected to represent a simple and ideal groundwater basin, this method can be applied to multiple spatial and time scales. Using these properties, specifically, the known hydraulic conductivity (K), the thickness of each layer (T_n), and the length of the system, it is possible to derive a set of equations that will produce an estimate of the residence time in each layer. By calculating a weighted average of the residence time of each layer, it is also possible to predict a system time. This system time can be considered the average residence time throughout the system. These equations do not require numerical modeling and an estimate can be done with a very low resolution of field site data.

The initial step is to determine the value and proportion of volumetric discharge that each layer contributes for vertically stratified hydraulic conductivity. This is achieved by rearranging Darcy's law to derive an equation solving for volumetric discharge in the x direction. However, because we are interested in determining an average discharge for each layer, the length over which the pressure drop occurs is not the length of the domain but is instead the length of the average flow path in each layer. The average flow path length for each layer is estimated by the sum of half the length of the domain and the thickness of the layer(s) through which it flows. It should be noted that a parcel of water traveling through the bottom layer must also travel through the top layer at the beginning and end of the flow path. Therefore, the estimation of the average flow path length of the bottom layer requires must take into account the total thickness of the domain. For this ideal basin geometry, the change in head over the width of the domain is 100m and is used for both the bottom and top layer calculations of an average volumetric discharge.

$$Q_1 = K_1 \cdot A_1 \cdot \frac{\partial h}{P_1} \tag{14}$$

$$Q_2 = K_2 \cdot A_2 \cdot \frac{\partial h}{P_2} \tag{15}$$

$$P_1 = \frac{1}{2}L + T_1 \tag{16}$$

$$P_2 = \frac{1}{2}L + T \tag{17}$$

$$T = T_1 + T_2 \tag{18}$$

The volumetric discharge calculations along with the estimation of the average flow path length for each layer make it possible to determine the time it takes a parcel of water to flow along the average flow-paths in the bottom and top layers. The equations are also a rearrangement of terms of Darcy's Law. However, we are now taking into account porosity to constrain the velocity of the fluid through the area of the domain. These times can be considered the average residence time in each of the layers.

$$\tau_1^* = \frac{P_1 \cdot n \cdot A_1}{Q_1} \tag{19}$$

$$\tau_2^* = \frac{P_2 \cdot n \cdot A_2}{Q_2} \tag{20}$$

Using the two average residence times from each layer, a weighted average calculation can be performed in order to determine the average residence time or system time. A weighted average must be used because the proportion of discharge that each layer contributes is not equal.

$$\tau^* = \frac{(\tau_1^* Q_1)+(\tau_2^* Q_2)}{Q_1+Q_2} \quad (21)$$

These calculations provide an estimate of mean residence time (τ*) in a groundwater system that is characterized by vertically stratified differences in hydraulic conductivity. Determining an average residence time for the system allows for the ability to normalize time when analyzing the flux of concentration of solute out of the system. Furthermore, this allows for comparison between cases of differing hydraulic conductivity furthering the ability to compare the evolution of the outflow concentration flux at specific relative (early or late) times.

4.4 Conservative Tracer Analysis

The combined initial steady-state model output with the addition of a conservative tracer to the system produces concentration data on both spatial and temporal scales. The data plotted in figure 4.6 show normalized concentration breakthrough curves as a function of time averaged over the outflow. Each simulation was run for the time necessary for the model to reach steady-state where C/C_0 is greater than 0.9999 throughout the entire domain. Figure 4.6 illustrates the different time scales for values of K_1 at which the domain becomes saturated with solute. For the case when K_1:K_2 is 1:1, the curve follows a normal increase in concentration with time reaching a normalized concentration of ~1 for the conservative tracer at the final time step. On the other hand, the case when K_1:K_2 is 100:1, the large proportion of volumetric flow delivered by the top

layer results in a much faster, relatively immediate increase in conservative tracer concentration. The subsequent slow increase of normalized concentration for the 100:1 case is a result of the bottom layer delivering conservative tracer to the outlet at later times. It should be noted that each simulation reaches a normalized concentration of ~1 due to stagnation zones that continue to deliver solute free water. In order to be able to compare the early and late time phenomenon that are occurring in each of the simulations, time was nondimensionalized by the average residence time calculated by using equation 21.

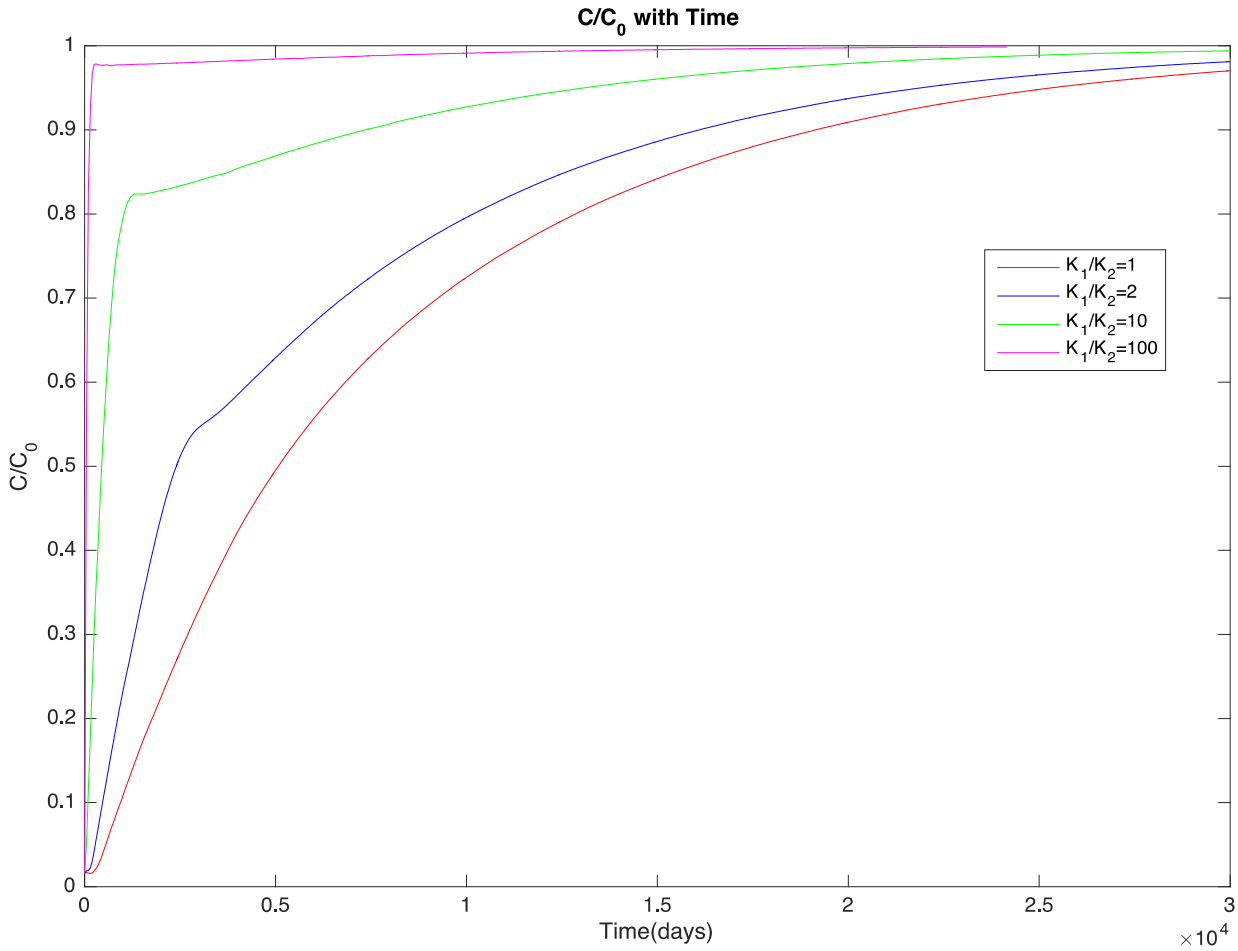

Figure 4.6: Conservative Tracer Breakthrough Curve from a Continuous Source.

As mentioned in Chapter 2., there are several methods that can be applied in order to normalize and nondimensionalize time scales when attempting to solve groundwater flow and solute transport problems. Figure 4.7 compares using a simplified column experiment approach to the Cardenas method and to the System Property method discussed in this text.

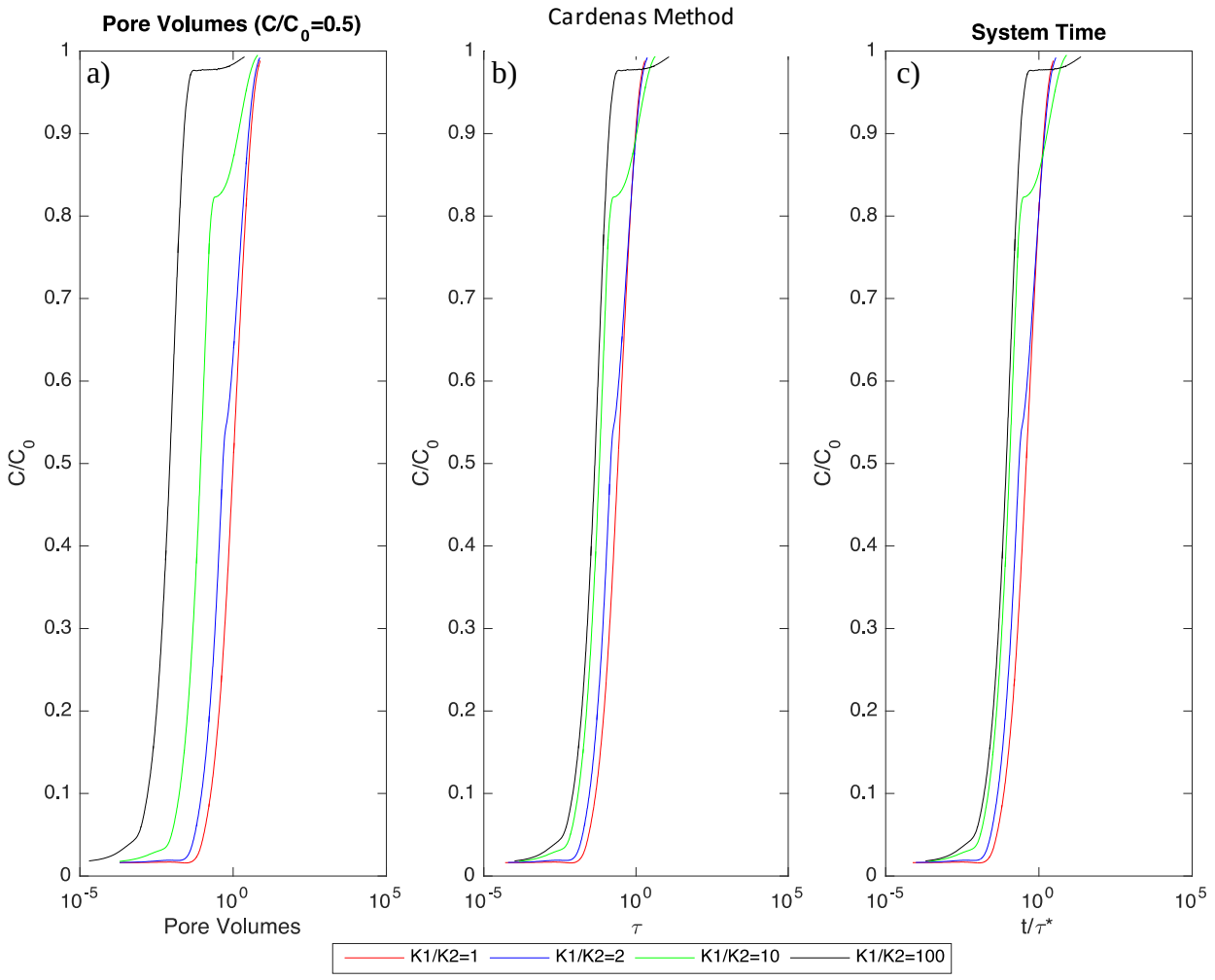

Figure 4.7: Comparison of Conservative Tracer Breakthrough Curves with Normalized Time. (a) Column Experiment Approach. (b) Cardenas Method. (c) System Property Method.

Figure 4.7a. uses the column experiment approach where the time needed for 1 pore volume to move through the system occurs when C/C_0 for a conservative tracer is equal to 0.5. For the purpose of this study, the time scales for all modeled cases were normalized against the time pore volume for the homogeneous case for figure 4.7a. The Cardenas method of nondimensionalizing time is illustrated in figure 4.7b. τ=1 is representative of the characteristic flushing time which can be calculated when equation 13 is rearranged to solve for time. In order to normalize time using this method, an average Darcy velocity was determined through each specific simulation. This resulted in four specific Darcy velocity values. The last method illustrated in figure 4.7c is the System Property method discussed in chapter 4.2. In this method, $1/\tau^{*}$=1 is representative of the mean residence time through the system; also defined as the characteristic system time. When compared to the Cardenas method, the System Property method plots very similarly for the entirety of the normalized time scales. For both methods, at relatively early times, when τ<1, the 100:1 case results in the earliest increase in concentration followed by each successive case where K_1:K_2 is less than 100:1. At relative early to intermediate times, both methods show breaks in the curves for all cases except the 1:1 case where the top layer has reached steady-state and now any change in concentration is a result of transport in the second layer. The breaks in the normalized time break through curves for the heterogeneous cases of hydraulic conductivity are a function of the proportion of volumetric flow in each layer. Therefore, it is possible to consider the following relationship:

$$\frac{Q_1(t)+Q_2(t)}{Q_T} \approx \frac{C}{C_0} \tag{22}$$

Where:

Q_t = Total Potential Volumetric Discharge (L^3t^{-1})

Equation 22 has the following relationship: at time t, the proportion of the sum of volumetric discharge contributed from each layer to the total amount of volumetric discharge that flows through the system is approximately equal to the the proportion of conservative tracer concentration that has been transported to the discharge area to the constant concentration at the recharge area. As a result of this relationship, the problem of vertically stratified differences in hydraulic conductivity can be considered one of superposition. In other words, the processes occurring in the two separate layers are cumulative resulting in a single signal.

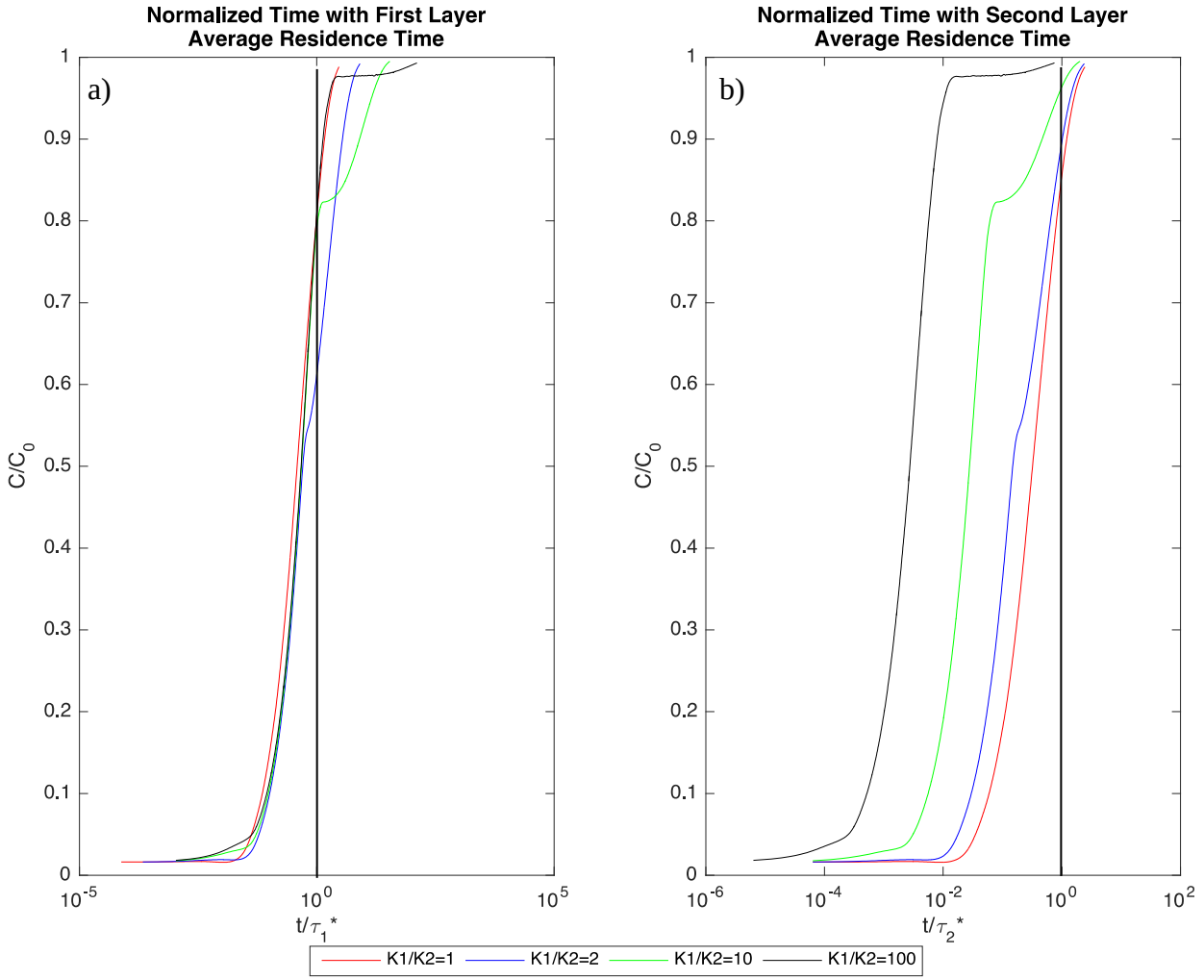

Figure 4.8: Breakthrough curves for a conservative tracer with normalized time based on a) top layer system time and b) bottom layer system time.

In order to decouple the two layers and determine differences in the relative contribution of solute from each layer for each case of K_1:K_2, it is necessary to normalize time based on the average mean residence time for each specific layer instead of the system time. Equations 19 and 20 are used to calculate the average residence time in each layer (τ_1^* and τ_2^* respectively) as a function of the average flow path distance, volumetric discharge from that layer, porosity, and the area of each layer.

Figure 4.8a uses τ_1^* in order to normalize time. When $t/\tau_1^*=1$, t=average residence time of the top layer. Therefore, the concentration of solute at the discharge area when $t/\tau_1^* \leq 1$has been transported through the top layer. All cases follow the same curve for early times indicating that the top layer is behaving as a result of the same flow characteristics. However, as stated in the discussion of equation 22, C/C_0 is related to Q/Q_T, resulting in a greater proportion of solute being transported in the top layer as K_1 increases relative to K_2.

Figure 4.8b uses τ_2^* in order to normalize time. When $t/\tau_2^*=1$, t=average residence time of the bottom layer. When $t/\tau_2^* \leq 1$, the concentration of solute at the discharge area has been transported through flow paths that have a residence time less than the average residence time in the bottom layer. It is for this reason that when $t/\tau_2^*>1$, solute is still being transported to the discharge area. Flow paths with a longer residence time than the average residence time as well as stagnation zones result in the transport of solute at much later times.

The set of equations that represent the System Time method can consequently be used to predict the proportion of a conservative tracer that is being transported from a recharge area to a discharge area through two vertically stratified layers with differences in hydraulic conductivity.

4.5 Reactive Transport Analysis

In order to evaluate the effects of vertically stratified differences in hydraulic conductivity on reactive transport of solute, selected rate constants cannot be arbitrary. Instead, the Damköhler number was employed to relate the reaction timescale to the advection timescale. The advection timescale can be considered the residence time for a conservative tracer of the system in question. As mentioned in chapter 3.4.2, a general rule of thumb for the Damköhler number is that when Da<<1, advection dominates and less solute in consumed and when Da>>1, the reaction rate is dominant and more than 90% of the solute is consumed. Using this general rule of thumb, two different Damköhler numbers were selected for the top layer for each case of K_1: 0.1 and 10 respectively. The Damköhler number in the bottom layer was held constant at 0.1. A Damköhler number of 0.1 was selected for the bottom layer based on the thermodynamic sequence of electron acceptors and the amount of energy obtained from each acceptor. Figure 4.9 shows this sequence for the oxidation of organic carbon in the saturated zone.

The oxidation of organic matter through oxygen as the electron acceptor yields the greatest amount of free energy to be used by the organism performing metabolism. In subsurface systems, organic carbon shows an exponential decrease in organic carbon with depth as a large suite of organisms perform aerobic respiration (Rosolen, 2014). Although there is the potential for metabolic processes that do not require organic carbon, such as autotrophic denitrification, these reactions occur a much slower rates (Pu, 2015). As a result, advection can be assumed to dominate at much greater depths in groundwater relative to reaction rates subsequently resulting in a smaller Damköhler number.

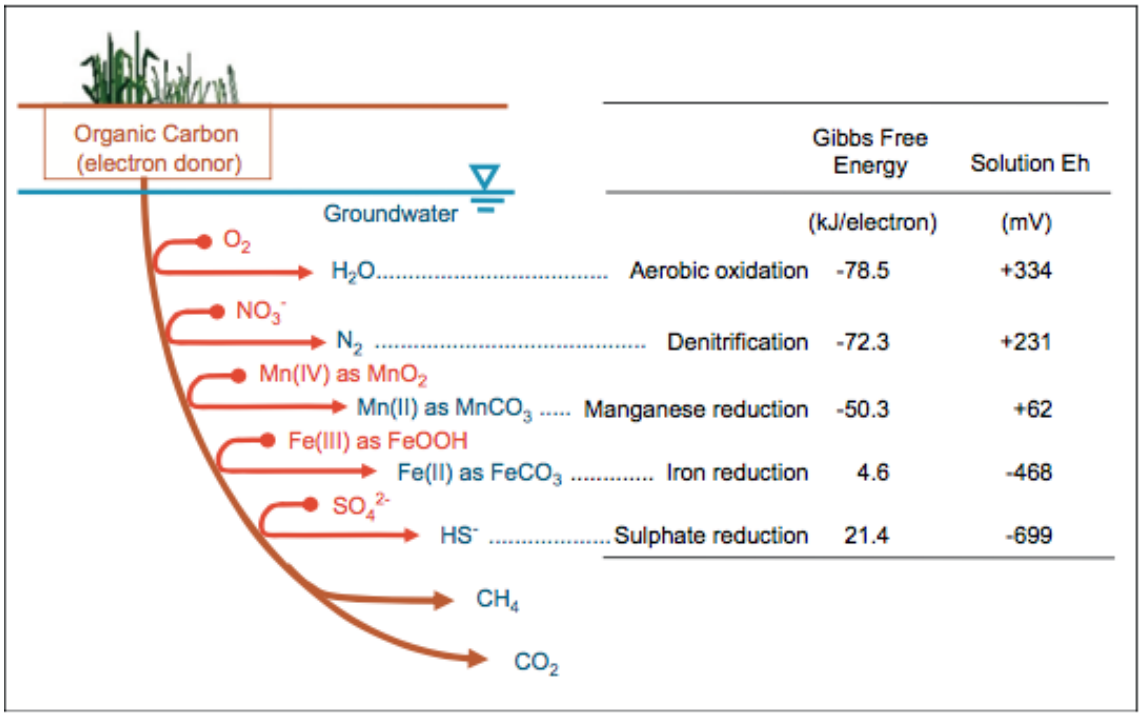

Figure 4.9: Thermodynamic sequence of electron acceptors for oxidation of organic carbon in the saturated zone (Rivett, 2008)

The same theoretical framework regarding the decrease in availability of electron donors and organic carbon substrate with depth was applied to the top layer. For the first scenario of reaction rate constants in the top layer, the Damköhler number was set to 0.1. This would indicate that most substrate and preferred electron donors are being consumed at very small depths. For the second scenario of reaction rate constants in the top layer, the Da was increased to 10. This would indicate an abundance of the necessary substrate for a specific reaction to move in the forward direction. It should also be noted that this same theoretical framework can be applied to reactions that may occur through abiotic processes. The reaction rates are also held constant in time throughout the simulation for a specific case of K_1 and Da_1 based on the

assumption that the amount of substrate, biotic conditions, and water chemistry conditions are all constant with time.

To calculate the reaction rate constants used for each case of K_1 when Da_1 is equal to 0.1 and 10, equation 11 was rearranged to solve for k as follows:

$$k = \frac{Da}{c_0^{n-1} \cdot \tau} \quad (23)$$

The initial concentration (c_0^{n-1}) was held at 1mol/m^3 for a first order reaction. τ was adjusted for the top layer residence times for each case of K_1 and each scenario of Da_1. This produces eight rate constant values that are shown in Table 4.1. The reaction rate constant for the bottom layer remains constant as Da_2 is held at 0.1 and no changes in mean residence time occur in the bottom layer.

Table 4.1: Reaction Rate Constants fore each Case of K_1 when Da_1 is 0.1 and 10 respectively and the Ratio of Top to Bottom Layer Rate Constants.

Da_1 = 0.1		
K_1(m/d)	*k_1 (1/d)*	*k_1/k_2*
0.1	*1.1E-05*	*1.7*
0.2	*2.2E-05*	*3.4*
1	*1.1E-04*	*17.0*
10	*1.1E-03*	*170.3*

Da_1 = 10		
K_1(m/d)	*k_1 (1/d)*	*k_1/k_2*
0.1	*1.1E-03*	*170.6*
0.2	*2.2E-03*	*341.2*
1	*1.1E-02*	*1705.9*
10	*1.1E-01*	*17058.8*

*Bottom Layer Rate Constant = 6.34E-06(1/d)

Simulations for each case of K_1 with the addition of reaction rates for the two scenarios of Da_1 were run for the same time period as the steady-state models. The amount of run time for each specific simulation was considered enough time for the simulations to reach steady-state.

The results for the Da_1 of 0.1 are plotted in figure 4.10. Time was normalized using the same method for the steady-state simulations; System Time method, first-layer normalization, and second layer normalization. The maximum C/C_0 value reached at steady-state was ~0.76. Only 24% of the total solute moving through the system is consumed through reactive processes. In order to distinguish between the top and bottom layers, time was normalized based on the calculated residence times for each layer from the steady-state simulations.

Figure 4.10b illustrates that for every case of K_1, when the Damköhler number in the top layer is 0.1, advection dominates, and minimal amount of solute consumption occurs in the top layer and a large concentration of solute is advected to the discharge area. Similar to the steady-state simulations, when $t/\tau_1^* \leq 1$ all solute that arrives at the discharge area has been transported through the top layer. The steep slope of the curves for each case of K_1 at relatively early times in figure 4.10b is another indicator that minimal consumption is taking place in the top layer.

Figure 4.10c has normalized time based on the calculated residence time of the bottom layer. At relatively late times when $t/\tau_2^* > 1$, C/C_0 has reached the maximum value stated above. This indicates that all flow paths that have a residence time less than the average residence time of the bottom layer have advected solute to the discharge area. Therefore, it is possible to consider that when the advective timescale dominates relative to the reactive timescale, consumption of solute only occurs in the system along flow paths that have a greater residence time than the average residence time in the bottom layer.

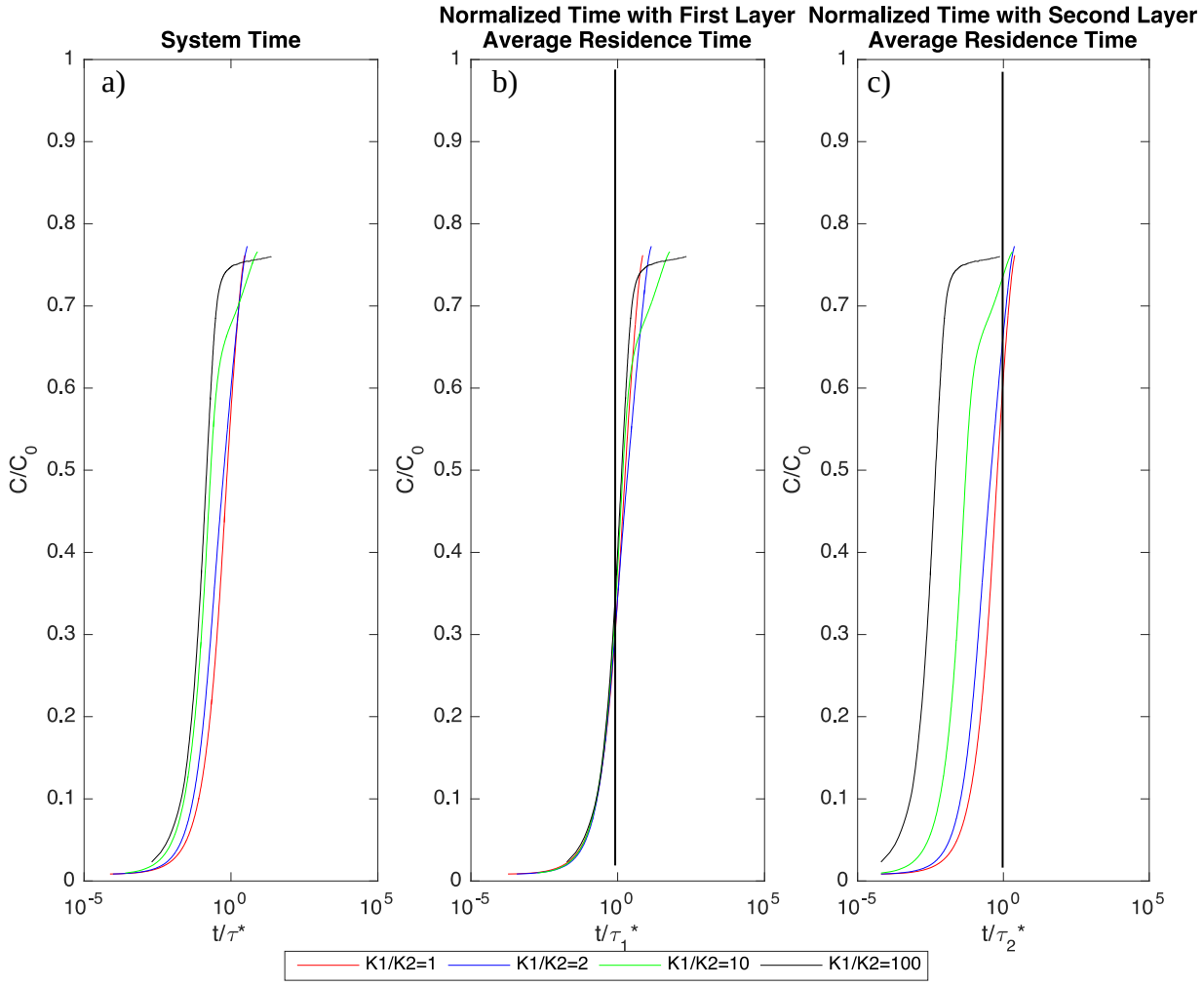

Figure 4.10: Breakthrough curves for the reactive case of Da_1=0.1 where time is normalized based on a) System Time, b)First layer residence time, and c) Second layer residence time.

The results for Da_1=10 are plotted in figure 4.11. Just as in the reactive transport simulation scenario where Da_1=0.1, time is normalized using the same method for the steady-state simulations; System Time method, first-layer normalization, and second layer normalization. The maximum C/C_0 reached when the simulation reached state state was ~0.036. This supports the Damköhler number general rule of thumb where Da>>1 results in >90% of the solute being consumed through reactive processes.

Figure 4.11b illustrates that for every case of K_1, when the Damköhler number in the top layer is 10, a large amount of consumption occurs in the top layer. Once again, when interpreting the evolution of concentration at the discharge area at early times when $t/\tau_1^* \leq 1$, there is an initial increase in solute concentration. This is due to the flow paths that have an infinitesimal residence time at the hinge points between the recharge and discharge areas. The system also reaches steady-state at a time much smaller than the average residence time in the top layer. This would further support that a large amount of solute consumption is occurring in the top layer.

Time was normalized based on the average residence time in the second layer and plotted in figure 4.11c. Similar to the scenario where Da_1=0.1, when $t/\tau_2^* >1$, C/C_0 has reached the maximum value stated above. However, unlike the scenario where Da_1=0.1, steady-state was reached at much earlier times for Da_1 =10. In this scenario, Da_2 is ten times smaller than Da_1. Therefore, any solute that is being transported through this second layer along flow paths that have a residence time $\approx \tau_2^*$ is being advected faster than it can be consumed in that layer. This further supports the notion that the majority of the consumption of solute is occurring

in the top layer. This would also indicate that solute that is transported through the bottom layer spends enough time in the top layer to be consumed.

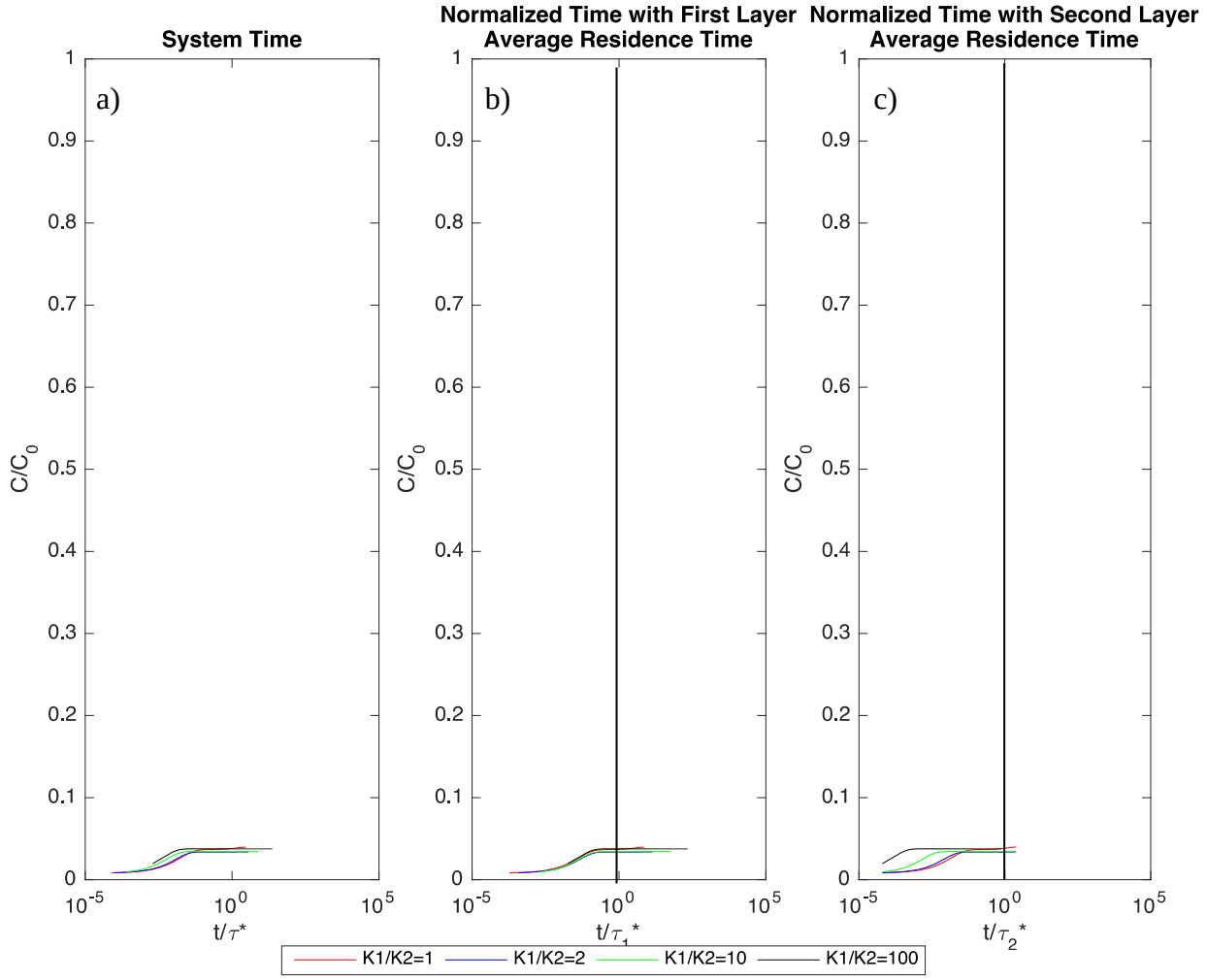

Figure 4.11: Breakthrough curves for the reactive case of Da_1=10 where time is normalized based on a) System Time, b)First layer residence time, and c) Second layer residence time.

It is imperative to discuss the relationship between the ratios of hydraulic conductivity in each layer, the Damköhler number, and reaction rate constants. The following discussion is in reference to table 4.1.

Reaction rate constants in this study were calculated based on the calculated residence times for each case in each layer using the System Time method. The hydraulic conductivity in the bottom layer is held constant for each case of varying K_1. As a result, the average residence time through the second layer is constant and by selecting a Damköhler number of 0.1 for this layer, the reaction rate constant in this layer remains constant as well for each simulation. In the first reactive transport scenario, Da_1=0.1 and the ratio of Damköhler numbers between the two layers is equal to 1. Therefore, the increase in reaction rate constant value in the top layer needed to meet a Damköhler number of 0.1 is proportional to the increase in hydraulic conductivity in the top layer. For example, when K_1:K_2=100:1, the reaction rate constant in the top layer is approximately 100 times greater than that in the bottom layer.

The second scenario for reactive transport used a Da_1=10 for the top layer in order to calculate the reaction rate constant. This results in the ratio of Damköhler numbers between the top and bottom layer being 100:1. If hydraulic conductivity is homogenous throughout the system, in order for the reaction rate constant in the first layer to be large enough to meet a Damköhler number of 10, it must be 100 times larger in the first layer relative to the second layer. For each successive case where K_1:K_2>1, the increase in reaction rate constant in the first layer is proportional to the product of the ratio of Damköhler numbers and the ratio of hydraulic conductivities between the first and second layer. For example, when K_1:K_2=100:1 and

Da_1:Da_2=100:1, the reaction rate constant in the top layer is 10^4 times larger than the reaction rate constant in the bottom layer. This relationship is represented in the following equation:

$$\frac{k_1}{k_2} \propto \frac{Da_1}{Da_2} \cdot \frac{K_1}{K_2} \tag{24}$$

Where:

k_1 =Reaction Rate Constant in the Top Layer (t^{-1})

k_2 =Reaction Rate Constant in the Bottom Layer (t^{-1})

Da_1 =Damköhler Number in the Top Layer

Da_2 =Damköhler Number in the Bottom Layer

K_1 =Hydraulic Conductivity in the Top Layer

K_2 =Hydraulic Conductivity in the Bottom Layer

Chapter 5. Conclusions and Recommendations.

5.1 Conclusions

The purpose of this study was to develop a conceptual and predictive framework for water and solute transport through an aquifer system that is vertically stratified with differences in hydraulic conductivity. In order to investigate this relationship, it was necessary to develop a method that provides an estimate of average residence time for the whole system as well as for each layer. This method is defined as the System Time Method and allows for the comparison of relative times between cases as well as the ability to decouple the system to better understand the contributions from each layer. By applying this method to a simple idealistic groundwater basin model, several important findings were discovered through the course of this study.

(1) **The System Time Method is a viable approach for estimating an average residence time a priori.** Using parameters that are intrinsic to the system in question allows the calculation of residence with minimal field data collection. When used to normalize time for a simulated transport model, the System Time method provides a similar ability as the method implemented by Cardenas to compare the behavior of breakthrough curves at relative times for the system as a whole.

(2) **Vertically stratified differences in hydraulic conductivity is a problem of superposition. The System Time method provides the ability to decouple the processes occurring in each layer.** By normalizing time based on the average residence time in a respective layer, it was possible to determine if different processes are occurring in that specific layer. For increasing values of hydraulic conductivity in the top layer, at relatively early times, the transport of solute in the top layer is similar to the homogenous

case. The differences arise from the relatively late time contribution from the second . Furthermore, for cases with greater hydraulic conductivity in the top layer, evolution of solute at the discharge area from the second layer will occur much later relative to the time it takes for solute to move through the top layer.

(3) Conservative tracer simulations provide an initial validation of the System Time Method. By normalizing time using the System Time method when simulating the transport of a conservative tracer through a system with vertically stratified differences in hydraulic conductivity, it was possible to determine the feasibility of the method. When normalizing time for each case by either the top or bottom layer average residence time, the proportion of concentration transported to the discharge area at each time is approximately equivalent to the proportion of the total volumetric discharge. For each case of K_1:K_2, at $t = \tau_2^*$, the proportion of volumetric discharge that has flowed through the system is approximately equal to 1. From figure 4.8, the concentration of solute that has been advected to the discharge area is also approximately equal to one. The addition of concentration after this time is due to flow paths that have a greater residence time than the average residence time in the bottom layer.

(4) The System Time Method coupled with reactive transport simulations provides a relationship between increasing hydraulic conductivity and the reaction rate constant necessary to achieve an amount of solute consumption. Two scenarios of the Damköhler number in the top layer were used. When the Damköhler number is homogeneous throughout the system (i.e Da_1=0.1), the reaction rate constant increase linearly with the differences in hydraulic conductivity between the top and

bottom layer and subsequently linearly with residence time. When the Damköhler number is greater in the top layer, the reaction rate necessary to achieve that level of solute consumption increases linearly with the product of the differences between the Damköhler number and the differences in hydraulic conductivity between the top and bottom layers.

5.2 Recommendations for Future Study

Future studies need to focus on validation of the System Time Method by conducting field experiments in areas with vertically stratified differences in hydraulic conductivity. These field studies should also be conducted for a conservative tracer as well as a contaminant of interest in the area. One potential application of this study is in regards to nitrate contamination. Natural nitrate attenuation occurs through heterotrophic and autotrophic denitrification at shallow and deeper depth respectively (Korom, 1992; Rivett et al., 2008). Due to the fact that these two metabolic pathways vary in rate of reactions, the System Time method could serve as a good estimate for the transport of nitrate through groundwater. Lastly, future studies will need to couple flow models to geochemical models that account for variability in substrate abundance, biotic community, and water conditions.

Bibliography

Alley, W. M., Healy, R. W., Labaugh, J. W., and Reilly, T. E. (2002). Flow and Storage in Groundwater Systems. *Science*, *296*, 1985–1990.

Cardenas, M. B. (2007). Potential contribution of topography-driven regional groundwater flow to fractal stream chemistry : Residence time distribution analysis of To ´ th flow. *Geophysical Research Letters*, *34*, 1–5.

Cardenas, M. B. (2008). Surface water-groundwater interface geomorphology leads to scaling of residence times. *Geophysical Research Letters*, *35*(April), 1–5.

Cardenas, M. B., and Jiang, X. W. (2010). Groundwater flow, transport, and residence times through topography-driven basins with exponentially decreasing permeability and porosity. *Water Resources Research*, *46*(11), 1–9.

Fitzgerald, Jonathan (2001). Field and Flow in Biological Systems: A word about Damköhler numbers. MIT.

Haggerty, R., Harvey, C. F., Freiherr von Schwerin, C., and Meigs, L. C. (2004). What controls the apparent timescale of solute mass transfer in aquifers and soils? A comparison of experimental results. *Water Resources Research*, *40*(1), 1–13.

Haggerty, R., McKenna, S. a, & Meigs, L. C. (2000). On the late-time behaviour of tracer breakthrough curves. *Water Resources Research*, *36*(12), 3467–3479.

Illangasekare, T., Ramsey, J., Jensen, K., and Butts, M. (1995). Experimental Study of Movement and Distribution of Dense Organic Contaminants in Hetergenous Aquifers. *Contaminant Hydrology*, (20), 1-25.

Jiang, X. W., Wan, L., Cardenas, M. B., Ge, S., and Wang, X. S. (2010). Simultaneous rejuvenation and aging of groundwater in basins due to depth-decaying hydraulic conductivity and porosity. *Geophysical Research Letters*, *37*(5), 1–5.

Jiang, X. W., Wan, L., Wang, X. S., Ge, S., and Liu, J. (2009). Effect of exponential decay in hydraulic conductivity with depth on regional groundwater flow. *Geophysical Research Letters*, *36*(24).

Korom, S. F. (1992). Natural Denitrification in the Saturated Zone,A Review, *28*(6), 1657–1668.

MacQuarrie, K. T. B., and Mayer, K. U. (2005). Reactive transport modeling in fractured rock: A state-of-the-science review. *Earth-Science Reviews*, *72*(3), 189–227.

Madhumitha Raghav, Susanna Eden, K., and Mitchell, B. W. (2013). Contaminants of Emerging Concern in Water Raise many questions.

Nolan, B.T. 2000. Relating nitrogen sources and aquifer susceptibility to nitrate in shallow wells of the United States. Ground Water, 39: 290-299.

Pu, J., Feng, C., Liu, Y., Li, R., Kong, Z., Chen, N. and Liu, Y. (2015). Pyrite-based autotrophic denitrification for remediation of nitrate contaminated groundwater. *Bioresource Technology*, *173*, 117–123.

Pye, V., and Kelley, J. (1984). The Extent of Groundwater Contamintation in the United States.*Groundwater Contamination, 23-35.*

Rivett, M. O., Buss, S. R., Morgan, P., Smith, J. W. N., and Bemment, C. D. (2008). Nitrate attenuation in groundwater: A review of biogeochemical controlling processes. *Water Research*, *42*(16), 4215–4232.

Rosolen, V., & Herpin, U. (2014). Hydromorphic Soil, Topographic Depression and Vegetation Development History by using 13C and 14C in Rondonia State (SW Brazillian Amazon) *33*(1), 136–146.

Rupp, D.E. and J.S. Selker. Drainage of a horizontal Boussinesq aquifer with a power-law hydraulic conductivity profile. Water Resour. Res. 41. DOI:10.1029/2005WR004241. 2005.

Saripalli K Prasad. (2002). Prediction of Diffusion Coefficients in Porous Media Using Tortuosity Factors Based on Interfacial Areas. *Ground Water*, *40*, 346–352.

Selker, J.S., J. Duan, and Y.-J. Parlange. Green and Ampt infiltration into soils of variable pore size with depth. Water Resour. Res. 35:1685-1688. 1999.

Steefel, C. I., DePaolo, D. J., & Lichtner, P. C. (2005). *Reactive transport modeling: An essential tool and a new research approach for the Earth sciences*. *Earth and Planetary Science Letters* (Vol. 240).

Toth, J. (1963). A Theoretical Analysis of Groundwater Flow in Small Drainage Basins'. *Journal of Geophysical Research*, *68*(15), 4795–4812.

USGS Websites (Updated 2016):
http://water.usgs.gov/nawqa/nutrients/pubs/wcp_v39_no12/,
http://water.usgs.gov/edu/earthwherewater.html,
http://toxics.usgs.gov/investigations/cec/index.php

Appendix A

Appendix A: Parameter Tables

This appendix contains tables of the parameters used to design the model used in this study.

Table A1. Parameter names, value, units, and description for model domain geometry.

Parameter	*Value*	*Units*	*Description*
z_0	*300*	*m*	*Height at Origin*
a	*50*	*m*	*Amplitude of Variations*
l_a	*1500*	*m*	*Wavelength of Periodic Topographic Variation*
b_0	*0*	*m*	*Base*
k	*1.00E-08*	m^2	*Permeability*
n	*0.2*		*Porosity*
df	*1.00E-05*	m^2/s	*Initial Dispersion Coefficient*
K_1	*See table*	*m/d*	*Hydraulic Conductivity Top Layer*
K_2	*0.1*	*m/d*	*Hydraulic Conductivity Bottom Layer*
k_1	*See table_*	*1/d*	*Rate Constant Top Layer*
k_2	*6.34E-06*	*1/d*	*Rate Constant Bottom Layer*

Table A2: Table of hydraulic conductivity values in the top layer.

Case	K_1*(m/d)*	K_1/K_2
1	*0.1*	*1:1*
2	*0.2*	*2:1*
3	*1*	*10:1*
4	*10*	*100:1*